Understanding confinement from deconfinement

M. Baker

Department of Physics, University of Washington, Box 351560, Seattle Washington 98195, USA
(Received 28 November 2007; revised manuscript received 4 June 2008; published 10 July 2008)

We use effective magnetic $SU(N)$ pure gauge theory with cutoff M and fixed gauge coupling g_m to calculate the nonperturbative magnetic response in the deconfined phase of $SU(N)$ Yang-Mills theory. We obtain the response to an external closed loop of electric current by reinterpreting and regulating the calculation of the one loop effective potential in Yang-Mills theory. This effective potential gives rise to a color magnetic charge density, the counterpart in the deconfined phase of color magnetic currents introduced in effective dual superconductor theories of the confined phase via magnetically charged Higgs fields. The resulting spatial Wilson loop has area law behavior. Using values of M and g_m determined in the confined phase, we find $SU(3)$ spatial string tensions compatible with lattice simulations in the temperature interval $1.5T_c < T < 2.5T_c$. Use of the effective theory to analyze experiments on heavy ion collisions will provide applications and further tests of these ideas.

DOI: 10.1103/PhysRevD.78.014009 PACS numbers: 12.38.Aw, 12.38.Mh

I. INTRODUCTION

The confined phase of $SU(N)$ Yang-Mills theory can be described by an effective theory coupling magnetic $SU(N)$ gauge potentials $\mathbf{C}_\mu$ to three adjoint representation Higgs fields [1]. The coupling of the potentials $\mathbf{C}_\mu$ to the magnetically charged Higgs fields generates color magnetic currents which, via a dual Meissner effect, confine Z_N electric flux to narrow tubes connecting a quark-antiquark pair [2]. The dual gluon (quanta of the magnetic gauge theory) acquires a mass M_g. For $SU(3)$, $M_g \sim 1.95\sqrt{\sigma}$ [3]. The effective theory is applicable at distances greater than the flux tube radius $R_{\rm FT} \sim \frac{1}{M_g} \sim 0.3$ fm. Since $SU(3)$ lattice simulations [4] yield a deconfinement temperature $T_c \approx 0.65\sqrt{\sigma}$, the scale $M_g \sim 3T_c$. There is then a range of temperatures within the interval $T_c < T < 3T_c$ where the effective theory should also be applicable in the deconfined phase. We will use the theory in this temperature range to calculate spatial Wilson loops, quantities that are outside the perturbative realm of finite temperature Yang-Mills theory.

In Sec. II we review the use of the effective theory in the confined phase. In Sec. III we describe the deconfined phase using the effective theory without Higgs fields, i.e. pure magnetic $SU(N)$ Yang-Mills theory with a cutoff M_g and gauge coupling constant g_m fixed by fits of heavy quark potentials in the confined phase [3].

In Sec. IV we show that the spatial Wilson loop of Yang-Mills theory is determined by the effective potential $U(C_0)$ of the magnetic theory in the background of a static dual scalar potential C_0. We evaluate the one loop contribution to $U(C_0)$ and use it to calculate spatial string tensions $\sigma_k(T)$ measuring magnetic flux with Z_N quantum number k passing through a large loop. We find that these string tensions are proportional to $k(N-k)$ (Casimir scaling), and that the predicted $SU(3)$ string tension is compatible with the results of lattice simulations [5] in the temperature range $1.5T_c < T < 2.5T_c$.

In Sec. V we compare $SU(N)$ lattice simulations of string tensions with lattice simulations [6] of dual string tensions $\tilde{\sigma}_k(T)$ (measuring Z_N electric flux) in the temperature range $T_c < T < 4.5T_c$. We find that the temperature $T \sim 1.5T_c$ marks a "transition" from a high temperature perturbative regime having $\tilde{\sigma}_k(T) > \sigma_k(T)$ to a low temperature domain where $\sigma_k(T) > \tilde{\sigma}_k(T)$.

In Sec. VI we compare the spatial string tension, calculated in the effective magnetic gauge theory, with that calculated [7] in the large N, large 't Hooft coupling limit of $SU(N)$ $\mathcal{N} = 4$ super Yang-Mills theory.

In the final section we summarize the results, discuss the significance of this work, and suggest extensions and further tests.

II. EFFECTIVE THEORY OF THE CONFINED PHASE

The effective theory describing the low energy excitations of $SU(N)$ Yang-Mills theory is a long distance dual $SU(N)$ Yang-Mills theory coupling non-Abelian magnetic $SU(N)$ gauge potentials $\mathbf{C}_\mu$ to 3 scalar fields ϕ_i, each in the adjoint representation of the magnetic gauge group. The Lagrangian $L_{\rm eff}$ has the form [1]

$$L_{\rm eff} = 2\,{\rm tr}[-\tfrac{1}{4}\mathbf{G}^{\mu\nu}\mathbf{G}_{\mu\nu} + \tfrac{1}{2}(D_\mu\phi_i)^2] - V(\phi_i), \quad (1)$$

where

$$\mathbf{G}_{\mu\nu} = \partial_\mu \mathbf{C}_\nu - \partial_\nu \mathbf{C}_\mu - ig_m[\mathbf{C}_\mu, C_\nu], \quad (2)$$

and

$$D_\mu\phi_i = \partial_\mu\phi_i - ig_m[\mathbf{C}_\mu, \phi_i]. \quad (3)$$

$V(\phi_i)$ is a Higgs potential which has a minimum at nonzero values of ϕ_i. It is chosen so that the Lagrangian (1)

describes a dual superconductor on the border between type I and type II.

In the confined phase the magnetic gauge symmetry is completely broken via a dual Higgs mechanism in which all particles become massive. (At least 3 adjoint scalars are necessary to completely break the symmetry.) The value ϕ_0 of the magnetic Higgs condensate is determined by the location of the minimum in the Higgs potential, and the dual (magnetic) gluon acquires a mass

$$M_g \sim g_m \phi_0 \tag{4}$$

via the dual Higgs mechanism.

The simplest possibility for the vacuum condensate $\langle \phi_i \rangle \equiv \phi_{i0}$ has the color structure [1]:

$$\phi_{10} = \frac{\phi_0}{\sqrt{2N}} J_x, \qquad \phi_{20} = \frac{\phi_0}{\sqrt{2N}} J_y, \qquad \phi_{30} = \frac{\phi_0}{\sqrt{2N}} J_z, \tag{5}$$

where J_x, J_y, and J_z are the three generators of the N dimensional irreducible representation of the three dimensional rotation group corresponding to angular momentum $J = \frac{N-1}{2}$. Since any matrix which commutes with all three generators must be a multiple of the unit matrix, there is no $SU(N)$ transformation which leaves all three ϕ_i invariant and the dual gauge symmetry is completely broken.

The excitations above the classical vacuum of the effective theory are flux tubes connecting a quark-antiquark pair in which Z_N electric flux is confined to narrow tubes of radius $\sim \frac{1}{M_g}$, at whose center the Higgs condensate vanishes. Explicit solutions have been obtained for $SU(3)$. The scale of the energy distribution in these electric flux tubes is determined by the dual gluon mass M_g. Since the effective theory describes fluctuations only at energy scales less than M_g, there is no physical excitation with this mass.

The effective theory has two parameters; g_m and M_g. Their values, $g_m \approx 3.91$ and $M_g \sim 800$ MeV, were determined [3] by comparing the predicted $SU(3)$ static heavy quark potential with lattice simulations. For distances $R > 0.3$ fm the lattice potential is well represented by the sum of a term linear in R and a $\frac{1}{R}$ term, $\frac{A_{\rm lattice}}{R}$ [8]. The value of g_m is obtained by writing the lattice $\frac{1}{R}$ potential in an effective Coulomb form:

$$\frac{A_{\rm lattice}}{R} = -\frac{4}{3}\frac{\pi}{g_m^2}\frac{1}{R}. \tag{6}$$

The right-hand side of (6) is the potential obtained by coupling magnetic gluons to a Dirac string connecting a quark-antiquark pair with a strength $\frac{2\pi}{g_m}$, which is the perturbative result of the effective theory. The coefficient of the linear potential is proportional to $\frac{M_g^2}{{g_m}^2}$ and determines the value of M_g in terms of σ and g_m.

The spin dependent and velocity dependent heavy quark potentials calculated with the above values of g_m and M_g [3] are compatible with results obtained from $SU(3)$ lattice simulations [9]. Furthermore, predicted energy distributions in electric flux tubes are compatible with lattice results for these distributions for values of R ranging from 1.0 fm down to 0.25 fm [10].

The long wavelength fluctuations of the axis of the electric flux tubes give rise to an effective bosonic string theory governed by the Nambu-Goto action [11]. These fluctuations are the low energy excitations of the effective theory. The value of g_m obtained from (6) includes the energy, $-\frac{\pi}{12R}$, of the long wavelength oscillations of the axis of the flux tube [12]. The value of $g_m \approx 3.91$ is close to 4, so that the main contribution to g_m comes from renormalization due to string fluctuations. Short distance fluctuations at energy scales greater than M_g do not enter in the effective theory, and g_m is the coupling constant defined at the fixed scale M_g.

III. THE EFFECTIVE THEORY IN THE DECONFINED PHASE

An approximate one loop calculation [13] of the finite temperature effective potential for the Higgs fields yielded a potential whose minimum moved to $\langle \phi_i \rangle = 0$ at a temperature $T \sim \phi_0$. The deconfinement temperature T_c is then on the order of ϕ_0. Above T_c the Higgs condensate vanishes, so the magnetic gluon becomes massless. However, since the deconfinement transition for $SU(N)$ groups with $N \geq 3$ is first order [4,14], the Higgs particles remain massive in the deconfined phase. (This first order phase transition was not seen in the calculation [13] since it did not include the contribution of a cubic term in the Higgs potential.)

We assume that away from the transition region the Higgs fields do not play an essential role in the deconfined phase, and we neglect them. The effective theory then reduces to a pure $SU(N)$ Yang-Mills theory of magnetic gauge potentials $\mathbf{C}_\mu \equiv (\mathbf{C}_0, \vec{\mathbf{C}})$. We will see that in the temperature interval $1.5T_c < T < 2.5T_c$ use of the pure gauge sector of the effective theory provides an understanding of features of the deconfined phase which parallels the use of the coupled gauge-Higgs theory to understand the confined phase. The pure gauge description breaks down at a temperature $T \sim \frac{M_g}{3} \sim T_c$. This breakdown can be regarded as a signal for the transition to the confined phase in the behavior of the pure gauge effective theory as the temperature is lowered toward T_c.

This theory has the same form as the microscopic electric theory, but with a fixed gauge coupling constant g_m and fixed ultraviolet cutoff M_g. The values of these two parameters are determined by the effective theory description of the confined phase. The magnetic gluons, which at $T = 0$ confine Z_N electric flux, become the physical degrees of freedom of the effective theory at $T > T_c$. These quanta are "strongly" interacting ($g_m \approx 3.91$), but their interaction is

cut off at distances less than 0.3 fm. Because of the duality between the microscopic electric $SU(N)$ Yang-Mills theory and the effective long distance magnetic $SU(N)$ gauge theory, perturbative calculations of electric quantities in the microscopic theory can be adapted to calculate magnetic quantities in the effective theory.

We can regard the magnetic Yang-Mills Lagrangian as the leading term in the long distance expansion of a dual effective Lagrangian, which in principle includes all powers of the magnetic gauge potentials $\mathbf{C}_\mu$ that maintain invariance under non-Abelian gauge transformations. This Lagrangian, if known exactly, would be the magnetic dual of the "electric" Yang-Mills Lagrangian. The infinite number of parameters in the dual Lagrangian reflects the fact that, in contrast with electrodynamics, where the dual Lagrangian $L(C_\mu)$ is just the Maxwell Lagrangian, an exact duality transformation from electric Yang-Mills potentials $\mathbf{A}_\mu$ to magnetic Yang-Mills potentials $\mathbf{C}_\mu$ is not known. In this paper we retain only the leading term in the dual Lagrangian, pure magnetic Yang-Mills theory, as an effective theory appropriate for calculating the long distance magnetic response in the deconfined phase of Yang-Mills theory.

The massless excitations of magnetic Yang-Mills theory having momenta less than the scale M_g must be integrated out (as in any effective theory) to obtain an effective action. We will see that the resulting one loop effective action $S_{\rm eff}$ generates a mass scale $\sim g_m T$. If this mass scale is greater than the cutoff M_g, higher loop corrections to $S_{\rm eff}$ can be neglected since there are no longer any propagating particles in the effective theory. Under such conditions we can use the one loop effective action $S_{\rm eff}$ at the classical level to determine the leading long distance behavior of spatial Wilson loops in the deconfined phase in the same manner that the Lagrangian (1) was used to evaluate temporal Wilson loops in the confined phase.

The ratio $\frac{M_g}{g_m T}$ plays the role of the expansion parameter in the effective theory. At the highest temperature $T \sim M_g$ where the effective theory should be applicable this parameter is of order $\frac{1}{g_m} = \frac{1}{3.91}$. (At $T = T_c$ it is close to unity.) Thus because of the relatively "large" value of g_m there is a range of temperatures within the interval $T_c < T < M_g$ where, in the leading long distance approximation, the one loop effective action can be treated at the classical level. Extension of the effective theory to higher mass scales would require calculating loop corrections to $S_{\rm eff}$ with the inclusion of additional interactions induced by the higher powers of the magnetic gauge potentials in the dual effective Lagrangian.

IV. THE SPATIAL WILSON LOOP CALCULATED IN THE MAGNETIC THEORY

To test the idea of using the effective theory to calculate magnetic quantities in the deconfined phase, we calculate spatial Wilson loops measuring magnetic flux with Z_N quantum number k passing through a loop L. (The spatial Wilson loop has area law behavior both above and below T_c.) The temporal Wilson loop of Yang-Mills theory determining the static heavy quark potential is obtained from the partition function of the effective dual theory in the presence of a Dirac string connecting a static quark-antiquark pair [1]. Similarly the spatial Wilson loop is obtained from the partition function of the effective magnetic theory in the presence of a current of k quarks circulating around the loop L. The current carried by the quarks is the source of a color magnetic field $\vec{\mathbf{B}}_k = \mathbf{G}_{0k}$, the magnetic analogue of the color electric field $\vec{\mathbf{E}}$ generated in the confined phase by the Dirac string [1]:

$$\vec{\mathbf{B}} = \vec{\nabla}\mathbf{C_0} - ig_m[\vec{\mathbf{C}}, \mathbf{C_0}] - \partial_t \vec{\mathbf{C}}. \tag{7}$$

To calculate the dual 't Hooft loop, we mirror the corresponding treatment [15–17] of the 't Hooft loop of Yang-Mills theory [18,19], replacing electric Yang-Mills theory by effective magnetic Yang-Mills theory. The spatial 't Hooft loop operator creates a closed line of magnetic flux along a loop L in Yang-Mills theory [18]. The corresponding dual 't Hooft operator creates a line of electric flux along L by implementing a singular magnetic gauge transformation $U = e^{i\Lambda(\vec{x})}$ which changes by a factor $e^{2\pi i(k/N)}$ when $\vec{x}$ traverses a closed path encircling the loop L. The expectation value of the dual 't Hooft operator measures the magnetic flux through L, and its effect on the partition function of the magnetic theory is to add to $\mathbf{C}_0$ an external potential $\mathbf{C}_0^{\rm Dirac} = \frac{T}{g_m}\Lambda(\vec{x})$.

For a single circulating quark (labeled j) we can take $\Lambda = \frac{\Omega_S(\vec{x})}{2}\mathbf{Y}_1^j$, where $\Omega_S(\vec{x})$ is the solid angle subtended at the point $\vec{x}$ by a surface S bounded by the loop L, and where $\mathbf{Y}_1^j$ is a diagonal matrix whose jth diagonal element is equal to $-\frac{(N-1)}{N}$ and whose remaining $N-1$ elements are equal to $\frac{1}{N}$. For k circulating quarks there are many representations of $SU(N)$ which carry k units of Z_N flux. Following the corresponding treatment of the 't Hooft loop [16], we couple the quarks in the completely antisymmetric representation. This yields [16]

$$\Lambda(\vec{x}) = \frac{\Omega_S(\vec{x})}{2}\mathbf{Y}_k, \tag{8}$$

where $\mathbf{Y}_k \equiv \sum_{j=1}^k \mathbf{Y}_1^j$ is a diagonal matrix having its first k elements equal to $-\frac{(N-k)}{N}$ and its remaining $N-k$ elements equal to $\frac{k}{N}$.

Linear combinations of the $N-1$ independent $SU(N)$ diagonal matrices could be used to construct corresponding gauge transformations Λ. For example, the matrix $\mathbf{Y}_k$ could have been replaced by the matrix $k\mathbf{Y}_1$. This would yield an operator creating k lines of electric flux along L, each containing one unit of Z_N flux. Use of a single configuration space function $C_0(\vec{x})$ having this color de-

pendence to search for a minimal action for the loop would yield a string tension $\sigma_k = k\sigma_1$, which is greater than the tension (24) obtained by seeking minimal action configurations proportional to $\mathbf{Y}_k$. This reflects the attraction between fundamental quark loops [16]. The choice of the antisymmetric representation in color space maximizes the effect of this attraction.

Equation (8) gives

$$\mathbf{C}_0^{\text{Dirac}}(\vec{x}) = \frac{2\pi T}{g_m}\frac{\Omega_S(\vec{x})}{4\pi}\mathbf{Y}_k, \tag{9}$$

which is the magnetostatic scalar potential of a steady current $\frac{2\pi T}{g_m}\mathbf{Y}_k$. (The total color charge transported along the loop L is $2\pi/g_m$ and the total elapsed Euclidean time is $1/T$.) The source of $\mathbf{C}_0^{\text{Dirac}}$ is a dipole layer $\vec{\mathbf{M}}(\vec{x})$ of magnetic charge lying in the surface S:

$$-\nabla^2\mathbf{C}_0^{\text{Dirac}} = \vec{\nabla}\cdot\vec{\mathbf{M}}(\vec{x}), \tag{10}$$

where

$$\vec{\mathbf{M}}(\vec{x}) = \frac{2\pi T}{g_m}\int_S d\vec{S}_y\,\delta(\vec{x}-\vec{y})\mathbf{Y}_k. \tag{11}$$

The gradient of $\mathbf{C}_0^{\text{Dirac}}(\vec{x})$ contains a term singular on the surface S defining Ω_S which is canceled by the contribution of $\vec{\mathbf{M}}$ to the magnetic field. The remaining regular part of $\vec{\nabla}\mathbf{C}_0^{\text{Dirac}}(\vec{x})$ gives the Biot-Savart magnetic field $\vec{B}_{\text{BS}}(\vec{x})$ of the current loop:

$$\begin{aligned}\vec{\nabla}\mathbf{C}_0^{\text{Dirac}}(\vec{x}) + \vec{\mathbf{M}} &= \frac{2\pi T}{g_m}\oint_L \frac{d\vec{y}\times(\vec{x}-\vec{y})}{4\pi|\vec{x}-\vec{y}|^3}\mathbf{Y}_k \\ &\equiv \frac{2\pi T}{g_m}\vec{B}_{\text{BS}}(\vec{x})\mathbf{Y}_k.\end{aligned} \tag{12}$$

The magnetic dipole layer $\vec{\mathbf{M}}$ generates the Biot-Savart field of a steady current, just as a Dirac string between static quarks generates the Coulomb field.

The partition function determining the dual 't Hooft loop can thus be obtained by the replacement $\vec{\nabla}\mathbf{C}_0 \to \vec{\nabla}\mathbf{C}_0 + \vec{\mathbf{M}}$ in the vacuum partition function, since minimizing the free action with this replacement yields both Poisson's equation (10) for $\mathbf{C}_0^{\text{Dirac}}(\vec{x})$ and the Biot-Savart magnetic field (12). The spatial Wilson loop of Yang-Mills theory, calculated in effective magnetic gauge theory, is then the partition function of the magnetic theory in the presence of the external source $\vec{\mathbf{M}}(\vec{x})$, divided by the vacuum partition function.

A. The effective potential $U(\mathbf{C}_0)$

To evaluate the partition function of the effective theory in the deconfined phase, where there is no classical potential, we must calculate the one loop effective potential $U(\mathbf{C}_0)$ of magnetic Yang-Mills theory in the background of a static magnetic scalar potential $\mathbf{C}_0$:

$$e^{-\int d\vec{x}\{[U(\mathbf{C}_0)]/T)\}} \equiv e^{-S^{1\text{-loop}}(\mathbf{C}_0)} = \det(-D^2_{\text{adj}}(\mathbf{C}_0)). \tag{13}$$

The effective potential $U(\mathbf{C}_0)$ is the counterpart in the deconfined phase of the classical Higgs potential generating electric flux tube solutions in the confined phase. The potential $U(\mathbf{C}_0)$ is a periodic function of the eigenvalues of $\mathbf{C}_0$ in the adjoint representation with period $2\pi T$, having minima at values of $\mathbf{C}_0$ for which the magnetic Polyakov loop is an element of Z_N. This potential gives rise to the spontaneous breakdown of the Z_N symmetry of the effective magnetic gauge theory in the deconfined phase.

We have evaluated $U(\mathbf{C}_0)$ integrating over the massless modes of magnetic Yang-Mills theory, introducing a Pauli-Villars regulator mass M to account for the short distance cutoff of the effective theory. The regulator mass M should be approximately equal to the dual gluon mass M_g determining the maximum energy of the modes included in the effective theory. Aside from the presence of the regulator, the calculation of $U(\mathbf{C}_0)$ mimics the calculation of the one loop effective potential $U(\mathbf{A}_0)$ in Yang-Mills theory [20,21] used to evaluate the spatial 't Hooft loop . We assume that the background potential $\mathbf{C}_0$ has the same Abelian color structure as $\mathbf{C}_0^{\text{Dirac}}$, i.e., $\mathbf{C}_0 = \frac{2\pi T}{g_m}C_0(\vec{x})\mathbf{Y}_k$. The corresponding effective potential $U(C_0)$ is then a periodic function of C_0 with period 1. The resulting expression for the one loop effective action $S^{1\text{-loop}}(C_0)$ is given by

$$S^{1\text{-loop}}(C_0) = \frac{k(N-k)(2\pi T)^2T^2}{3g_m^2}\int d\vec{x}\frac{U(C_0)}{T}, \tag{14}$$

where

$$U(C_0) = \left[[C_0]^2(1-[C_0])^2 - \frac{3}{4\pi^4}I\left(C_0,\frac{T}{M}\right)\right], \tag{15}$$

and

$$I\left(C_0,\frac{T}{M}\right) = \int_0^\infty dy y^2\log\left(\frac{\cosh\sqrt{y^2+(\frac{M}{T})^2}-\cos(2\pi C_0)}{\cosh\sqrt{y^2+(\frac{M}{T})^2}-1}\right), \tag{16}$$

with $[C_0] \equiv |C_0|_{\text{mod }1}$. The factor $2k(N-k)$ is the number of nonzero eigenvalues of the matrix $\mathbf{Y_k}$ in the adjoint representation [16]. The integral $I(C_0,\frac{T}{M})$ reflects the presence of the Pauli-Villars regulator in the functional determinant (13), which suppresses the short distance contribution to $U(C_0)$.

The one loop effective potential is ultraviolet finite, so that in the absence of a regulator ($M \to \infty$), $I \to 0$. In this limit the expression (15) reduces to $U(A_0)$, with C_0 replaced by A_0 and g_m replaced by the running Yang-Mills coupling constant $g(T)$. In contrast with the effective theory, the one loop expression for $U(A_0)$ contains modes of all wavelengths and is applicable only at high temperatures where $g(T) \to 0$ so that the contribution of higher order

loops are small. In the magnetic theory there are no higher loop corrections to $U(C_0)$ in the leading long distance approximation, not because the coupling constant g_m is small, but because it is an effective theory in which only modes having masses greater than the cutoff can propagate.

It is convenient to separate the background scalar potential C_0 into the contribution $\frac{\Omega_S}{4\pi}$ of the external source and a remaining contribution c_0 whose sources are the magnetic charges of the plasma:

$$C_0 = c_0 + \frac{\Omega_S}{4\pi}. \tag{17}$$

Then making the replacement (17) in $S^{\text{1-loop}}$ and adding the classical action using (12) gives the effective action $S_{\text{eff}}(c_0)$:

$$S_{\text{eff}}(c_0) = \frac{4\pi^2 Tk(N-k)}{Ng_m^2}\int d\vec{x}\Big[(\vec{\nabla}c_0 + \vec{B}_{\text{BS}})^2 + U\Big(c_0 + \frac{\Omega_S}{4\pi}\Big)\frac{Ng_m^2T^2}{3}\Big]. \tag{18}$$

The scalar potential c_0 is subject to the conditions $c_0(\vec{x}) \to 0$ for $\vec{x}$ on L, and $c_0(\vec{x}) \to -\frac{\Omega_S(\vec{x})}{4\pi}$ as $\vec{x} \to \infty$. The latter condition means that the total magnetic field $\vec{B}(\vec{x}) = \vec{\nabla}c_0 + \vec{B}_{\text{BS}}$ is short range, decaying to its vacuum value at large distances from the loop. $S_{\text{eff}}(L)$, the minimum value of $S_{\text{eff}}(c_0)$, determines the spatial Wilson loop, $e^{-S_{\text{eff}}(L)}$, as calculated in the effective theory.

The term in (18) linear in $\vec{B}_{\text{BS}}$ is a surface term which, because of the boundary condition that c_0 vanishes on L, gives no contribution to S_{eff}. The term quadratic in $\vec{B}_{\text{BS}}$, the magnetic energy of a current loop, diverges logarithmically as the thickness of the wire goes to zero. (For a thin wire of radius a this energy is proportional to $L\log\frac{L}{a}$.) After separating off this Biot-Savart energy, the first term in (18) becomes simply $(\vec{\nabla}c_0)^2$. Then only the second term in (18) along with the boundary at large distances involve the external potential explicitly.

Because of the periodicity property of the effective potential, $U(C_0) = U(C_0 + 1)$, the value of $U(c_0 + \frac{\Omega_S}{4\pi})$ is independent of the choice of the surface S defining the solid angle $\Omega_S(\vec{x})$, and we can choose S to be the plane surface bounded by the loop L. For a square loop of side L in the xy plane centered at the origin

$$\Omega_S(x,y,z) = -\int_{-(L/2)}^{L/2} dx' \int_{-(L/2)}^{L/2} dy' \times \frac{z}{[(x-x')^2 + (y-y')^2 + z^2]^{3/2}}. \tag{19}$$

Since $U(-C_0) = U(C_0)$ and $\Omega_S(x,y,-z) = -\Omega_S(x,y,z)$, in minimizing (18) we can consider configurations $c_0(x,y,z)$ which are odd functions of z so that $c_0 = 0$ at $z = 0$ for all x and y and the boundary condition on the loop is then automatically satisfied.

The minimization of $S_{\text{eff}}(c_0)$ yields "Poisson's equation" for c_0:

$$-\nabla^2 c_0(\vec{x}) = \rho_{\text{mag}}(\vec{x}), \tag{20}$$

where

$$\rho_{\text{mag}}(\vec{x}) \equiv -\frac{1}{2}\frac{Ng_m{}^2T^2}{3}\frac{dU(c_0 + \frac{\Omega_S}{4\pi})}{dc_0} \tag{21}$$

is the color magnetic charge density induced in the vacuum by the current loop. This charge produces a field screening $\vec{B}_{\text{BS}}$, so that the total field $\vec{B}(\vec{x})$ has an exponential falloff determined by the "Debye" screening mass $m_{\text{mag}}(T)$ of the magnetic theory:

$$m_{\text{mag}}^2(T) = \frac{1}{2}\frac{d^2U(C_0)}{dC_0^2}\Big|_{C_0=0}\Big(\frac{Ng_m^2T^2}{3}\Big). \tag{22}$$

The dual screening mass $m_{\text{mag}}(T)$ determines both the width of the magnetic energy profile surrounding a large spatial Wilson loop in the deconfined phase and the long distance behavior of magnetic charge density correlators. (Since there is no local relation between electric and magnetic variables in non-Abelian gauge theory, the magnetic charge density (21) should correspond to an extended quantity in Yang-Mills theory.)

Using Eqs. (15), (16), and (22), we plot $\frac{m_{\text{mag}}(T)}{M}$ in Fig. 1 as a function of $\frac{T}{T_c}$ for $SU(3)$. We note that for $T > T_c$, $m_{\text{mag}}(T) > M$, so that $m_{\text{mag}}(T)$ is not a physical excitation of the effective theory in the deconfined phase just as M_g is not a physical excitation in the confined phase. Thus for $T > T_c$, in the leading long distance approximation there are no propagating particles present in the effective theory to correct the effective action and the classical field distribution $\vec{B}(\vec{x})$ obtained from the one loop effective potential.

However, as T is lowered to temperatures below $\frac{M}{3}$, where the width $\frac{1}{m_{\text{mag}}(T)}$ of the magnetic profile function

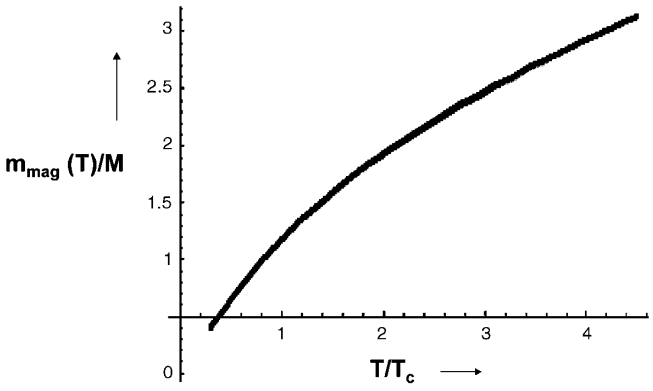

FIG. 1. Ratio of dual screening mass to the regulator mass M as a function of $\frac{T}{T_c}$ for $SU(3)$, with $T_c = \frac{M}{3}$ and $g_m = 3.91$.

becomes larger than the minimum wavelength $\frac{1}{M}$ of the fluctuations included in the effective theory, the classical solution is no longer valid. This breakdown of the pure gauge effective theory at lower temperatures is a signal for the transition to the confined phase for which the Higgs fields play an essential role.

B. Spatial string tension: Comparison with $SU(3)$ lattice simulations

For large L the effective action of the dual theory has area law behavior determining the spatial string tension $\sigma_k(T)$:

$$S_{\rm eff}(L) \to L^2 \sigma_k(T), \quad \text{as } L \to \infty. \tag{23}$$

The spatial string tension is the interface energy separating two vacua of magnetic $SU(N)$ gauge theory differing by k units of Z_N charge. The calculation of $\sigma_k(T)$ follows closely the corresponding calculation [21] of the dual spatial string tension $\tilde{\sigma}_k(T)$, the interface energy in Yang-Mills theory.

We first take the limit $L \to \infty$ in (20) and (21). In this limit the scalar potential $c_0 = c_0(z)$ and the magnetic field $\vec{B} = \vec{B}(z)$ are functions only of the distance z from the loop. Furthermore, the solid angle $\Omega_S = -2\pi$ for $z > 0$ and 2π for $z < 0$, so that the boundary condition $C_0 \to 0$ at large distances becomes $c_0(z) \to \pm\frac{1}{2}$ as $z \to \pm\infty$. In Fig. 2 we plot $\vec{B}^2(z)$ at $T = \frac{M}{3}$, obtained by solving (20) with these boundary conditions.

Evaluating $S_{\rm eff}(c_0)$ at the "classical" solution $c_0(z)$ yields

$$\frac{\sigma_k(T)}{T^2} = \frac{4\pi^2 k(N-k) F(\frac{T}{M})}{3 g_m \sqrt{3N}}, \tag{24}$$

where

$$F\left(\frac{T}{M}\right) \equiv 6 \int_{-(1/2)}^{1/2} dc_0 \sqrt{U\left(c_0 + \frac{1}{2}\right)}. \tag{25}$$

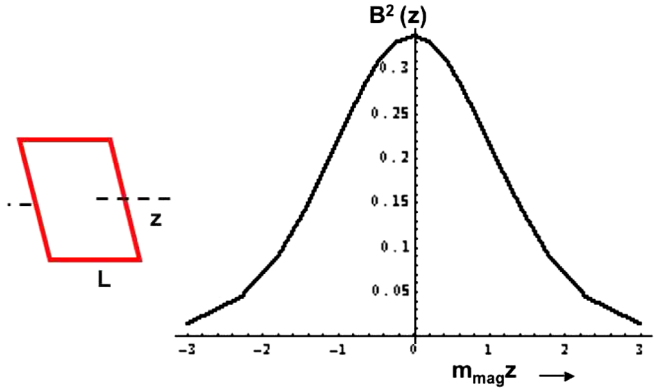

FIG. 2 (color online). Magnetic energy density profile $\vec{B}^2(z)$ at $T = T_c$ as a function of distance z from L.

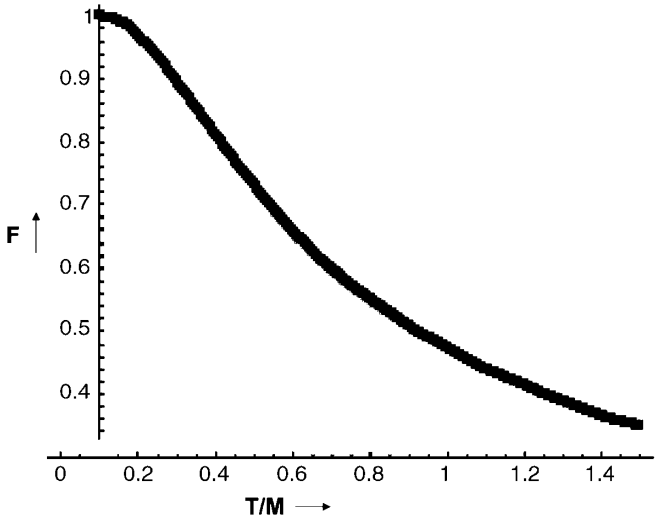

FIG. 3. Function $F(\frac{T}{M})$, defined in (25), arising from a Pauli-Villars regulator mass M, suppressing short distance contributions to the string tensions $\sigma_k(T)$.

Equation (24) is applicable for any $SU(N)$ group, but the values of g_m and M have been determined only for $SU(3)$ where the effective theory has been applied in the confined phase. The function $F(\frac{T}{M})$, plotted in Fig. 3, is the ratio of the action with regulator mass M to the unregulated action. The temperature dependence of the ratio $\frac{\sigma_k(T)}{T^2}$ comes from the Pauli-Villars cutoff, which suppresses the contributions of momenta greater than M to $\sigma_k(T)$. Since the Pauli-Villars regulator is rather "soft," allowing substantial contributions from momenta greater than M, we have also evaluated the string tension using values of M smaller than M_g.

In Fig. 4 we plot $\frac{T}{\sqrt{\sigma(T)}}$ for $SU(3)$ ($k = 1$, $\sigma_k \equiv \sigma$) as a function of $\frac{T}{T_c}$ for Pauli-Villars masses $M = 800$, 700, and 600 MeV, and compare with the results of 4D lattice

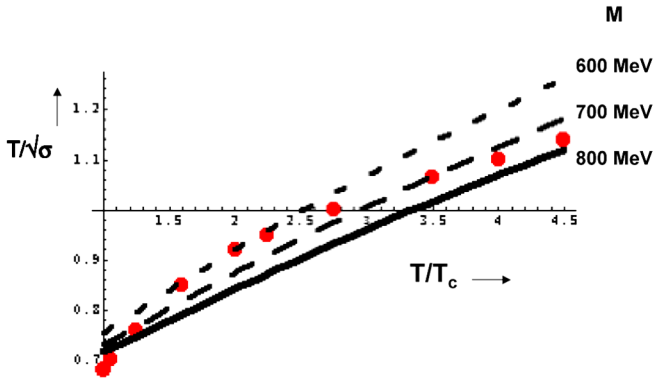

FIG. 4 (color online). Comparison of $SU(3)$ 4D lattice data (dots) [5,22] for the spatial string tension $\sigma(T)$ with the prediction (24) of the effective magnetic Yang-Mills theory, for three values of the Pauli-Villars regulator mass M.

simulations [5,22]. We note the following features of these curves:

(i) At $T \approx T_c$ the predicted values of $\frac{T}{\sqrt{\sigma(T)}}$ lie close to the lattice result, and they increase as the temperature increases, reflecting the decrease with temperature of the function $F(\frac{T}{M})$ due to the Pauli-Villars regulator.

(ii) $M = 600$ MeV gives the best fit to the $SU(3)$ lattice data in the temperature interval $1.5T_c < T < 2.5T_c$ where the effective theory should be applicable.

(iii) The value of the string tension does not depend strongly on the Pauli-Villars mass. (This reflects the ultraviolet finiteness of the one loop effective potential.)

(iv) The lattice data in Fig. 4 are fit very well almost down to T_c by combining the nonperturbative value of the string tension of 3D $SU(3)$ Yang-Mills theory (determining the high temperature limit of the 4D string tension) with the 2-loop calculation of the running of the coupling constant $g_E(T)$ of a three-dimensional effective theory (EQCD) determining the change in the spatial string tension as the temperature is lowered [22]. By contrast, the effective dual theory determines the string tension in the deconfined phase only in a limited low temperature range, but uses parameters already determined in the confined phase. The values of the intercepts of the curves in Fig. 4, which are determined primarily by the value $g_m \approx 3.91$, are predictions of the effective theory. For example, for $SU(8)$ and $k = 1$, Eq. (24) with $M \to \infty$ gives $\frac{\sqrt{\sigma_1}}{T} \approx 1.72$, while $SU(8)$ lattice simulations close to $T = T_c$ [14] give $\frac{\sqrt{\sigma_1}}{T} \approx 1.63$.

C. Spatial string tension $\sigma_k(T)$: Casimir scaling

We note from (24) that $\sigma_k(T)$ is proportional to $k(N-k)$ (Casimir scaling). This dependence on the quantum number k of spatial string tensions in the deconfined phase is consistent with the results of lattice simulations of $SU(4)$, $SU(6)$, and $SU(8)$ gauge theories [14,23]. [In the confined phase only the $SU(3)$ string tension was calculated in the effective theory, so that no prediction regarding Casimir scaling can be made.]

Casimir scaling of the spatial string tension has also been obtained in a model of the deconfined phase as a gas of non-Abelian monopoles in the adjoint representation [23,24].

V. SPATIAL STRING TENSIONS AND DUAL STRING TENSIONS COMPARED

In Fig. 5 we compare the $SU(3)$ lattice data for the string tension with data for dual string tensions $\tilde{\sigma}_k(T)$ measured in lattice simulations of $SU(3)$, $SU(4)$, $SU(6)$, and $SU(8)$ gauge theory in the temperature range $T_c < T < 4.5T_c$ [6].

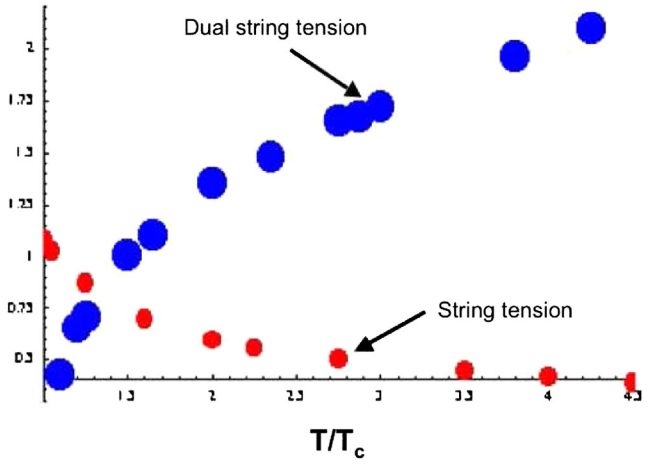

FIG. 5 (color online). Comparison of dual string tension and string tension lattice data. Large dots: $SU(N)$ data ($N = 3, 4, 6$, and 8) for dual string tensions $\frac{\tilde{\sigma}_k}{T^2}$, divided by the Casimir factor $k(N-k)$, as a function of $\frac{T}{T_c}$ [19]. Small dots: Same plot of $SU(3)$ data for $\frac{\sigma}{2T^2}$ [5].

The lattice data for $\frac{\tilde{\sigma}_k(T)}{T^2}$ for all these $SU(N)$ groups and for all possible values of k, when scaled by the Casimir factor $k(N-k)$, all collapse on a single curve $\frac{\tilde{\sigma}(T)}{T^2}$ shown by the large dots in Fig. 5 . This approximate Casimir scaling of dual string tensions agrees with the two loop perturbative prediction [16]. (The Casimir scaling of this two loop result holds approximately for the three loop calculation [17], where it is violated by a small amount.)

At $T \approx 4.5T_c$ the magnitude $\tilde{\sigma}(T)$ of the dual string tension agrees with the two loop perturbative prediction, but at lower temperatures it is suppressed [6] relative to this prediction. This temperature range, where nonperturbative effects on dual string tensions becomes significant, closely corresponds to the temperature range where the spatial string tension becomes comparable to the dual string tension. To show this, in Fig. 5 we also plot $\frac{\sigma(T)}{2T^2}$, using the $SU(3)$ string tension lattice data in Fig. 4. We see that at $T \approx 4.5T_c$ the string tension $\sigma(T) \sim 0.2\tilde{\sigma}(T)$ and that, as the temperature decreases, $\frac{\sigma(T)}{T^2}$ increases, becoming greater than $\frac{\tilde{\sigma}(T)}{T^2}$ for temperatures less than $T \sim 1.25T_c$.

We can then identify three temperature intervals in the deconfined phase, each having distinctly different electric and magnetic responses according to the value of the ratio $\gamma(T)$:

$$\gamma(T) = \frac{\sigma_k(T)}{\tilde{\sigma}_k(T)}. \tag{26}$$

(i) $T > 4.5T_c$, $\gamma(T) < 1$: The dual string tension is perturbatively calculable, and the effective magnetic theory cannot be used to calculate the string tension ($T \geq M$).

(ii) $1.5T_c < T < 2.5T_c$, $\gamma(T) \sim 1$: The dual string tension is suppressed relative to its perturbative value, and the spatial string tension is calculable via the effective magnetic theory [$T < M < m_{\rm mag}(T)$].

(iii) $T_c < T < 1.5T_c$, $\gamma(T) > 1$: Neither perturbation theory nor the effective magnetic theory are applicable. In this temperature range $m_{\rm mag}(T) \sim M$, which is a signal for the transition to the confined phase.

VI. SPATIAL STRING TENSION: COMPARISON WITH $\mathcal{N} = 4$ SUPER YANG-MILLS THEORY

In this section we compare the string tension predicted by the effective magnetic theory with the expression $\sigma_{\rm SYM}(T)$ for the spatial string tension of $SU(N)$ $\mathcal{N} = 4$ super Yang-Mills theory, calculated in the large N limit and in the limit of large 't Hooft coupling $\lambda \equiv g^2_{\rm SYM}N$, where the gravity-conformal field theory correspondence is applicable [7]:

$$\sigma_{\rm SYM}(T) = \frac{\pi}{2}\sqrt{\lambda}T^2. \tag{27}$$

There is no scale in $\mathcal{N} = 4$ SYM theory, λ is a free parameter, and the theory remains in the deconfined phase at all temperatures with $\frac{\sigma_{\rm SYM}}{T^2} = \frac{\pi}{2}\sqrt{\lambda}$.

In the scale free limit, $M \to \infty$, the one loop result of the effective magnetic theory $\frac{\sigma_k(T)}{T^2}$ is also constant. In this limit $F(\frac{T}{M}) = 1$ and (24) becomes

$$\sigma_k(T) = \frac{4}{3\sqrt{3}}\frac{\pi}{2}\sqrt{\lambda_m}\frac{k(N-k)}{N}T^2, \tag{28}$$

where

$$\lambda_m \equiv \left(\frac{2\pi}{g_m}\right)^2 N \tag{29}$$

is the 't Hooft coupling of the effective magnetic theory. Equation (28) is applicable for any $SU(N)$, but the value of λ_m is known only for $SU(3)$ where $g_m = 3.91$ gives $\sqrt{\lambda_m} = 2.78$.

The factor $\sqrt{\lambda_m}$ in (28), determining $\sigma_k(T)$ in magnetic $SU(N)$ Yang-Mills theory, is proportional to the width $\frac{1}{m_{\rm mag}(T)}$ of the magnetic profile multiplied by the number N of unit Z_N charges in the large N limit. The factor $\sqrt{\lambda}$ in (27), determining $\sigma_{\rm SYM}$, arises from the relation between the 't Hooft coupling and the fundamental string scale via the AdS/CFT correspondence.

The limit $N \to \infty$ of (28) gives the factorized form:

$$\sigma_k(T) \to k\sigma_1(T) = k\frac{4}{3\sqrt{3}}\frac{\pi}{2}\sqrt{\lambda_m}T^2. \tag{30}$$

Since the string tensions $\sigma_{\rm SYM}(T)$ and $\sigma_1(T)$ [(27) and (30)] have the same dependence on the 't Hooft couplings of the two theories, the corresponding string tensions will be equal if these two constants are related by a numerical factor of order unity. That is, imposing the relation

$$g_{\rm SYM} = \frac{4}{3\sqrt{3}}\frac{2\pi}{g_m}, \tag{31}$$

between the coupling constants g_m and $g_{\rm SYM}$ of the two theories, we obtain the equality of the two string tensions:

$$\sigma_{\rm SYM}(T) = \sigma_1(T). \tag{32}$$

That is, with the correspondence (31) the spatial string tension $\sigma_{\rm SYM}(T)$ is equal to the interface tension $\sigma_1(T)$ of magnetic $SU(N)$ gauge theory calculated with the one loop effective potential. This correspondence provides a link between effective magnetic Yang-Mills theory and $\mathcal{N} = 4$ supersymmetric Yang-Mills theory.

VII. SUMMARY

We have shown that effective magnetic $SU(N)$ Yang-Mills theory can be used in the one loop approximation to calculate long distance magnetic properties of the deconfined phase, in analogy to the use of the effective magnetic theory in the classical approximation to describe the confined phase.

Calculating the one loop effective potential for C_0 with an ultraviolet cutoff M, we find:

(i) At $T = \frac{M}{3} \sim T_c$ the width of the magnetic energy profile (Fig. 2) is approximately equal to the radius of the $T = 0$ electric flux tube.

(ii) In the temperature interval $1.5T_c < T < 2.5T_c$ the predicted $SU(3)$ spatial string tension is compatible with lattice simulations (Fig. 4).

(iii) In this temperature interval the values of the string tension and the dual string tension obtained from lattice simulations (Fig. 5) approach each other and become equal as the temperature is lowered to about $1.25T_c$. Roughly speaking, the temperature scale $M \sim 3T_c$ marks a transition in the behavior of the deconfined phase; the high temperature domain is described by perturbative Yang-Mills theory and the low temperature interval by the effective magnetic gauge theory.

(iv) For $SU(N)$ groups with $N \geq 3$ the string tensions $\sigma_k(T)$ satisfy Casimir scaling.

(v) With the duality correspondence (31) the spatial string tension $\sigma_{\rm SYM}(T)$, calculated in $\mathcal{N} = 4$ SYM theory, is equal to string tension $\sigma_1(T)$, calculated in the effective magnetic theory in the scale free limit.

VIII. DISCUSSION

The formation of the magnetic energy profile around a spatial Wilson loop in the deconfined phase parallels formation of an electric flux tube in the confined phase.

In the confined phase a Dirac string connecting a quark-antiquark pair couples to the magnetic vector potential $\vec{C}$

and induces a magnetic color current density brought about by the interaction of the gauge potentials with the magnetically charged Higgs fields. Via the dual of Ampere's law, this current density gives rise to an electric field $\vec{E} = -\vec{\nabla} \times \vec{C}$ which screens the external Coulomb field generated by the Dirac string, so that the total color electric field decays exponentially with the energy profile of an electric flux tube.

In the deconfined phase a magnetic dipole layer couples to the magnetic scalar potential C_0 and induces a magnetic color charge density (21) generated by the one loop effective $U(C_0)$. Via the dual of Gauss's law, this magnetic charge density gives rise to a magnetic field $\vec{B} = \vec{\nabla} c_0$ which screens the external Biot-Savart magnetic field generated by the dipole layer, so that the total magnetic field decays exponentially at large distances and has the energy profile shown in Fig. 2.

We thus gain an understanding of confinement by studying the deconfined phase. The magnetic currents confining electric flux, introduced at the classical level via Higgs fields, are the counterparts in the confined phase of magnetic charges, generated in the deconfined phase by integrating out the long distance quantum fluctuations of the non-Abelian magnetic degrees of freedom. As the temperature is lowered toward T_c, the classical magnetic energy profile resulting from the one loop pure gauge effective action becomes unstable, signaling the transition to the confined phase where the Higgs fields must be taken into account.

In the confined phase the long wavelength fluctuations of the axis of the flux tubes give rise to an effective bosonic string theory and consequently to the $-\frac{\pi}{12R}$ Lüscher correction to the area law behavior of Wilson loops. In contrast, in the deconfined phase there is no Higgs condensate whose zeros locate the position of the string, and consequently no effective string theory. Instead, in order to calculate the corrections to the area law behavior of spatial Wilson loops in the deconfined phase in the temperature range where the effective theory is applicable, we must solve (20) for finite values of L and evaluate the corresponding effective action (18). This calculation will be described in a separate paper.

IX. FURTHER INVESTIGATIONS

Finally, we suggest the following tests and applications of the effective magnetic gauge theory.

(i) According to our picture, the magnetic response of the plasma phase of $SU(N)$ Yang-Mills theory in the temperature interval $1.5T_c < T < 2.5T_c$ is described by effective magnetic $SU(N)$ gauge theory. In this temperature range the deconfined phase contains magnetic charges interacting strongly ($g_m \sim 3.91$) over distances greater than 0.3 fm, according to the effective action (18). Since such temperatures are accessible in heavy ion collisions, calculations of nonequilibrium quantities in the effective theory would make it possible to use the magnetic description of the long distance properties of the plasma phase of Yang-Mills theory to analyze these experiments.

(ii) Evidence for the magnetic quanta of the effective theory should be sought in lattice simulations of Yang-Mills theory in the deconfined phase. We could make use of the recent proposal [25] to identify the magnetic component of the plasma phase of Yang-Mills theory with monopole currents which wind around the temperature direction and whose density can be extracted from lattice simulations [26–28]. Spatial correlations of these wrapped monopoles [28] could then be compared with correlators of the magnetic charge density (21) determined by the effective theory.

ACKNOWLEDGMENTS

I would like to thank O. Aharony, B. Bringoltz, M. Chernodub, Ph. de Forcrand, M. Fromm, A. Karch, C. P. Korthals Altes, A. Vuorinen, and L. Yaffe for their valuable help.

[1] M. Baker, J. S. Ball, and F. Zachariasen, Phys. Rev. D **44**, 3328 (1991).
[2] S. Mandelstam, Phys. Rep. **23C**, 245 (1976); G. 't Hooft, *Proceedings of the European Physical Society Conference, Palermo, 1975*, edited by A. Zichichi (Editrice Compositori, Bologna, 1976).
[3] M. Baker, J. S. Ball, and F. Zachariasen, Phys. Rev. D **56**, 4400 (1997).
[4] B. Lucini, M. Teper, and U. Wenger, Phys. Lett. B **545**, 197 (2002).
[5] G. Boyd, J. Engels, F. Karsch, E. Laermann, C. Legeland, M. Lütgemeier, and B. Petersson, Nucl. Phys. **B469**, 419 (1996).
[6] Ph. de Forcrand, B. Lucini, and D. North, Proc. Sci., LAT2005 (2006) 323 [arXiv:hep-lat/0510081v1].
[7] A. Brandhuber, N. Itzhaki, J. Sonnenschein, and S. Yankielowicz, J. High Energy Phys. 06 (1998) 001.
[8] O. Kaczmarek and F. Zantow, Phys. Rev. D **71**, 114510 (2005).
[9] G. S. Bali, K. Schilling, and A. Wachter, Phys. Rev. D **56**,

2566 (1997).
[10] A. M. Green, C. Michael, and P. S. Spencer, Phys. Rev. D **55**, 1216 (1997).
[11] M. Baker and R. Steinke, Phys. Lett. B **474**, 67 (2000); Phys. Rev. D **63**, 094013 (2001); **65**, 094042 (2002).
[12] M. Lüscher, Nucl. Phys. **B180**, 317 (1981).
[13] M. Baker, J. S. Ball, and F. Zachariasen, Phys. Rev. Lett. **61**, 521 (1988).
[14] B. Lucini, M. Teper, and U. Wenger, J. High Energy Phys. 02 (2005) 033.
[15] C. P. Korthals Altes, A. Kovner, and M. Stephanov, Phys. Lett. B **469**, 205 (1999).
[16] P. Giovannangeli and C. P. Korthals Altes, Nucl. Phys. **B608**, 203 (2001).
[17] P. Giovannangeli and C. P. Korthals Altes, Nucl. Phys. **B721**, 1 (2005); **B721**, 25 (2005).
[18] G. 't Hooft, Nucl. Phys. **B138**, 1 (1978); **B153**, 141 (1979).
[19] Ph. de Forcrand, M. d'Elia, and M. Pepe, Phys. Rev. Lett. **86**, 1438 (2001).
[20] D. Gross, R. D. Pisarski, and L. Yaffe, Rev. Mod. Phys. **53**, 43 (1981).
[21] T. Bhattacharya, A. Gocksch, C. P. Korthals Altes, and R. D. Pisarski, Nucl. Phys. **B383**, 497 (1992); Phys. Rev. Lett. **66**, 998 (1991).
[22] Y. Schröder and M. Laine, Proc. Sci., LAT2005 (2006) 180 [arXiv:hep-lat/0509104v1].
[23] C. P. Korthals Altes and H. Meyer, arXiv:hep-ph/0509018v1.
[24] C. P. Korthals Altes, arXiv:hep-ph/0408301v1.
[25] M. N. Chernodub and V. I. Zakharov, Phys. Rev. Lett. **98**, 082002 (2007).
[26] V. G. Bornyakov, V. K. Mitrjushkin, and M. Muller-Preussker, Phys. Lett. B **284**, 99 (1992).
[27] S. Ejiri, Phys. Lett. B **376**, 163 (1996).
[28] A. D'Alessandro and M. D''Elia, arXiv:0711.1262v2.